Molecular Therapy
Methods & Clinical Development
Original Article

Antibodies to recombinant human alpha-L-iduronidase prevent disease correction in cortical bone in MPS I mice

Sarah C. Hurt,[1] Steven Q. Le,[1] Shih-hsin Kan,[2] Quang D. Bui,[3] Michael D. Brodt,[1] and Patricia I. Dickson[1]

[1]Washington University School of Medicine, St. Louis, MO 63110, USA; [2]Children's Hospital of Orange County, Orange, CA 92868, USA; [3]The Lundquist Institute for Biomedical Innovation, Torrance, CA 90502, USA

Mucopolysaccharidosis I (MPS I) is a lysosomal storage disorder caused by deficiency of the enzyme α-L-iduronidase (IDUA). Failure of enzyme replacement therapy (ERT) to treat skeletal disease may be due to development of anti-IDUA antibodies, found previously to alter tissue distribution of ERT in animal models. To test this hypothesis, immunocompromised (non-obese diabetic [NOD]-severe combined immunodeficiency [SCID]) MPS I mice were treated with weekly ERT from birth (ERT alone). Some mice also received weekly injections of rabbit immunoglobulin G (IgG) against IDUA (immunized rabbit immune globulin [IRIG]) concomitant with ERT, imitating antibodies developed in patients (ERT+IRIG). Mice treated with ERT+IRIG showed lower IDUA activity and higher disease burden than mice treated with ERT alone in most tissues. Femora were harvested at 20 weeks for *ex vivo* microcomputed tomography (μCT). Femoral cortical bone thickness and cortical bone area in MPS I mice were greater than in unaffected mice. Mice treated with ERT alone had values that were statistically indistinguishable from carrier mice, while mice that received ERT+IRIG had no significant differences compared to vehicle-treated MPS I mice. The data suggests that immune-modulatory or immune-suppressive therapy to prevent or reduce the humoral immune response against ERT may improve treatment of skeletal disease due to MPS I.

INTRODUCTION

Mucopolysaccharidoses I (MPS I) is a lysosomal storage disorder caused by a deficiency in activity of α-L-iduronidase (IDUA) leading to a lack of breakdown of heparan and dermatan sulfate glycosaminoglycans (GAGs) and a broad range of devastating clinical outcomes, including skeletal deformities.[1] Skeletal manifestations of MPS cause impaired mobility and diminished quality of life for patients.[2] Thoracolumbar gibbus, stiff joints, and short stature are some of the many skeletal manifestations of MPS I that are overall referred to as dysostosis multiplex.[1,3,4] The skeletal disease is a major untreated burden of MPS I; even patients who receive enzyme replacement therapy (ERT) and/or hematopoietic stem cell transplantation require additional treatment, such as physical therapy and surgical intervention for the musculoskeletal aspects of the disease.[1,3,5–7]

Up to 90% of patients receiving intravenous (i.v.) ERT with recombinant human IDUA (rhIDUA) develop antibodies against it.[8–13] Due to the rhIDUA being perceived as foreign to the patient's immune system, it is unsurprising that a patient would have an immune response to the large quantities of normal enzyme given at a single administration.[14] In clinical trials, participants treated with ERT for MPS I, MPS II, MPS VI, and Fabry and Pompe diseases developed humoral immune responses to the recombinant enzymes, which were predominantly immunoglobin G (IgG).[14–17] Previous preclinical studies have shown that the humoral immune response that occurs as a result of ERT may reduce the effectiveness of this treatment.[8,18] Our previous study has shown that (immune-competent) MPS I mice that received weekly i.v. ERT from 4–16 weeks of age that developed anti-IDUA antibodies showed an altered tissue distribution of the enzyme compared to mice that did not develop antibodies.[18] The humoral immune response to ERT has been explored previously in MPS I dogs, where it was found that ERT failed to prevent GAG accumulation and pathology in synovium and cartilage of adult dogs that developed anti-IDUA antibodies during the treatment period. Dogs treated with immune suppression and ERT showed improved penetration and correction of joint and cartilage compared to those with antibodies. We studied MPS I dogs treated with ERT beginning in the first month of life. We found normal to near-normal skeletal morphology in these dogs; the dogs did not develop anti-IDUA antibodies during treatment. Thus it is possible that, in addition to the impact of early initiation of therapy, the lack of an immune response to ERT was at least partly responsible for the improved distribution and efficacy of ERT in these dogs.[19] Similarly, mice do not generate an immune response when treated with ERT from birth, complicating the ability to separately study the impact of an immune response and the impact of timing of the initiation of treatment.[20] Furthermore, while mice and dogs that receive ERT at birth do not mount a humoral immune response to the enzyme, the same does not appear to be true for human patients.[8–10,14,18,19] MPS I patients are not routinely

Received 28 February 2024; accepted 30 December 2024;
https://doi.org/10.1016/j.omtm.2024.101405.

Correspondence: Patricia I. Dickson, 4444 Forest Park Avenue, Street 5400, St. Louis, MO 63108, USA.
E-mail: pdickson@wustl.edu

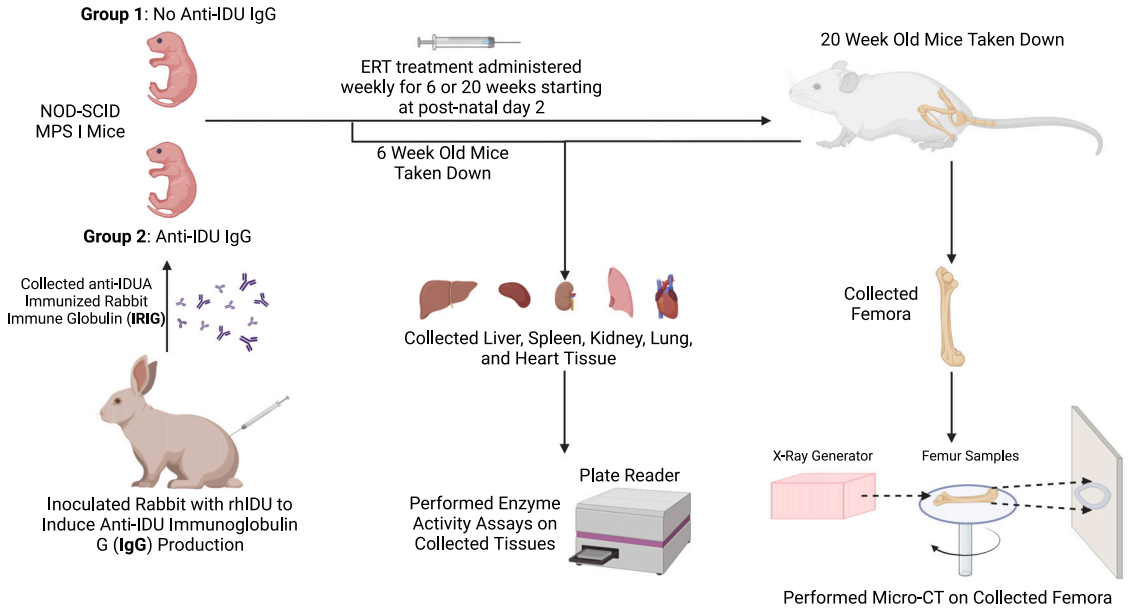

Figure 1. Outline of the study design

Rabbits were previously inoculated with rhIDUA to induce anti-IDUA IgG production. The anti-IDUA IgG purified from serum (IRIG) of these animals was collected and used in the current study by i.p. injecting one group of NOD-SCID MPS I mice with IRIG before administering each i.v. ERT dose. NOD-SCID MPS I mice were treated weekly with i.v. ERT with or without IRIG for 6 or 20 weeks starting on postnatal day 2.

immune suppressed when ERT is initiated. Therefore, it is essential to study whether initiation of early ERT, even in the presence of a humoral immune response against the enzyme, might be sufficient to prevent skeletal manifestations, as suggested previously.[21–23]

We designed an experiment to isolate the antibody-related effect from that of early treatment. Previously, we immunized rabbits against rhIDUA, harvested their serum, and demonstrated that this immunized rabbit immune globulin (IRIG) inhibited the uptake of rhIDUA into MPS I fibroblasts.[18] Here, we administered ERT beginning at birth to immunocompromised MPS I mice in the non-obese diabetic (NOD)-severe combined immunodeficiency (SCID) background in the presence or absence of IRIG (Figure 1).[24] This design permitted the study of the effects of early ERT in MPS I mice with and without IgG antibodies against rhIDUA. To maximize the potential effect of ERT in the presence or absence of anti-IDUA antibodies, we treated mice weekly with 1.57 mg/kg body weight, which is higher than the typical dose of 0.58 mg/kg that is used clinically.[19] We found significant differences in the distribution of ERT as measured by IDUA activity and the reduction of tissue β-hexosaminidase (β-hex) activity, which is secondarily elevated in MPS I and serves as a marker for lysosomal storage.[25,26] We further performed *ex vivo* microcomputed tomography (μCT) on femora collected at 20 weeks and found no improvement in cortical bone structure in the ERT+IRIG group compared to untreated MPS I controls, whereas the ERT-alone group showed a normal cortical bone structure. The results suggest that even high-dose ERT from birth is insufficient to normalize cortical bone structure in the presence of a humoral immune response against rhIDUA in MPS I mice.

RESULTS

IRIG alters ERT distribution in NOD-SCID MPS I mice

The animals used in this study, untreated MPS I (knockout [KO]) mice, unaffected carrier mice, and MPS I mice received weekly ERT alone or received ERT+IRIG from birth, as summarized in Table 1. To confirm that administration of IRIG to NOD-SCID MPS I mice resulted in a measurable antibody titer against rhIDUA *in vivo*, serum samples from the 6-week cohort were collected, and specific rabbit

Table 1. Experimental groups

Group name	Genotype	6-week study (*N*)	20-week study (*N*)	μCT (*N*)	ERT (mg/kg)	IRIG (mg/kg)
Carrier	+/−	7	13	6	0	0
KO	−/−	3	11	3	0	0
ERT+IRIG	−/−	5	10	9	1.57	22
ERT	−/−	5	11	11	1.57	0

KO mice are saline-injected NOD-SCID MPS I mice. Carrier mice are saline-injected NOD-SCID mice that are heterozygous carriers for MPS I (*Idua*$^{+/-}$). ERT mice are NOD-SCID MPS I mice treated with weekly i.v. ERT(1.57 mg/kg) from birth. ERT+IRIG are NOD-SCID MPS I mice treated with weekly i.p. rabbit IgG against rhIDUA (22 mg/kg) prior to i.v. ERT (1.57 mg/kg) from birth. μCT, microcomputed tomography; *N*, number of mice in each group. Only a subset of mice had their femora collected, so the *N* for μCT reflects how many femora were assayed in each group.

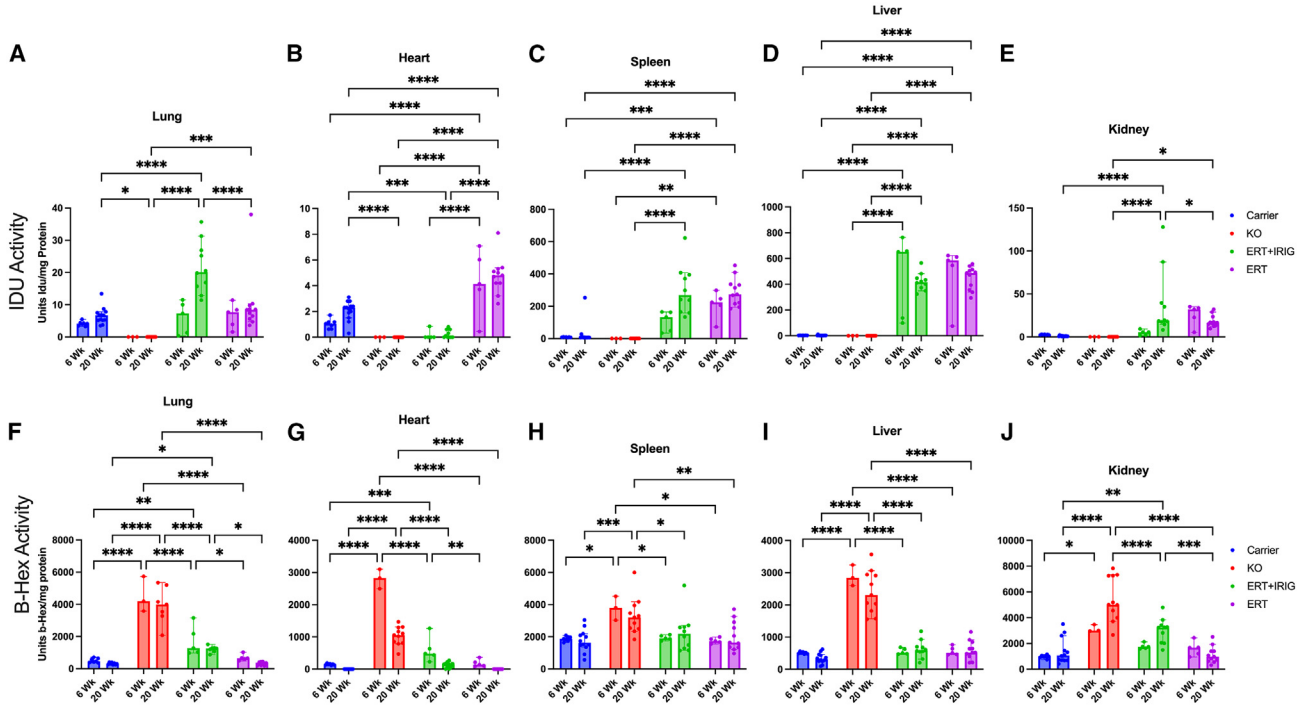

Figure 2. IDUA and β-hex enzyme activity assays at end of study from mice sacrificed at 6 or 20 weeks of age

(A–J) Carrier, saline-injected carrier NOD-SCID mice (blue); KO, saline-injected NOD-SCID MPS I mice (red); ERT+IRIG, NOD-SCID MPS I mice treated with IRIG and weekly i.v. ERT (green); ERT, NOD-SCID MPS I mice treated with weekly i.v. ERT alone (purple). $^{*}p < 0.05$, $^{**}p < 0.01$, $^{***}p < 0.001$, $^{****}p < 0.0001$. Each dot represents the measurement from an experimental animal, and bars symbolize the median value with a 95% confidence interval (CI). Please note differences in scale on the y axis.

IgG titers were quantified by ELISA in these serum samples We found, as we expected, that only the ERT+IRIG group had a rabbit anti-IDUA IgG antibody titer (median 47.7 optical density units/μL serum). To determine whether these exogenously produced rabbit anti-IDUA antibodies may have interfered with the distribution of ERT (as we found in studies of a naturally occurring immune response),[18] we assayed IDUA enzymatic activity in organs harvested at necropsy at 6 weeks and 20 weeks of age, 24 h following the final weekly ERT dose (Figures 2A–2E). The ERT+IRIG group had significantly more IDUA activity than the ERT-alone group in the lungs, liver, and kidneys at 20 weeks (Figures 2A, 2D, and 2E), which have resident tissue macrophages and reticuloendothelial cells, whereas in the heart, we found significantly higher levels of IDUA activity in mice treated with ERT alone compared to mice treated with ERT+IRIG at both 6 and 20 weeks (Figure 2B). We further studied the correlation between rabbit anti-IDUA IgG in mouse serum and tissue IDUA activity within the ERT+IRIG group at 6 weeks of age (Figure 3). We found a negative correlation between IDUA activity and rabbit anti-IDUA IgG antibody titers that reached statistical significance for the lungs, spleen, and liver (coefficient of determination [R^2]: 0.9480, 0.8742, 0.9310; $p = 0.0051$, 0.0197, and 0.0079) (Figures 3A, 3C, and 3D). Notably, except for a single sample, no detectable IDUA activity was found in the heart of the 6-week-old animals (Figures 2B and 3B). The one animal receiving IRIG in addition to ERT that was observed to have uptake in the heart had very low levels of IDUA activity that did not exceed average carrier levels (Figures 2B and 3B).

Activity of the enzyme β-hex is increased in MPS I mice, and its normalization is used as a treatment-responsive indicator of improvement in lysosomal storage in the mice.[25,27,28] We assayed the organs of MPS I mice treated with ERT or ERT+IRIG and controls for β-hex activity at 6 weeks or 20 weeks of age, 24 h after the final ERT dose (Figures 2F–2J). At both time points, activity of β-hex was lower in all organs in both treatment groups (ERT+IRIG and ERT alone) compared to KO controls (Figures 2F–2J). When comparing the two treatment groups to each other, the ERT-alone group had a lower β-hex activity in the heart at 6 weeks compared to the ERT+IRIG group ($p < 0.01$) (Figure 2G). At 20 weeks of age, we found significantly lower β-hex activity in the lungs (median: 370.6 β-hex units/mg protein) and kidneys (median: 967.6 β-hex units/mg protein) in the ERT-alone group compared to levels in the ERT+IRIG group (median lungs: 1260.2 β-hex units/mg protein, median kidneys: 3240.2 β-hex units/mg protein) (Figures 2F and 2J). Additionally, in the kidneys, while we saw a reduction in IDUA activity in mice treated without antibodies when looking from our 6-week cohort to our 20-week cohort (Figure 2E), we still saw significantly lower levels of β-hex activity in the 20-week group when compared to mice given ERT and antibodies (Figure 2J). The liver and spleen generally have more reticuloendothelial cells that take up more

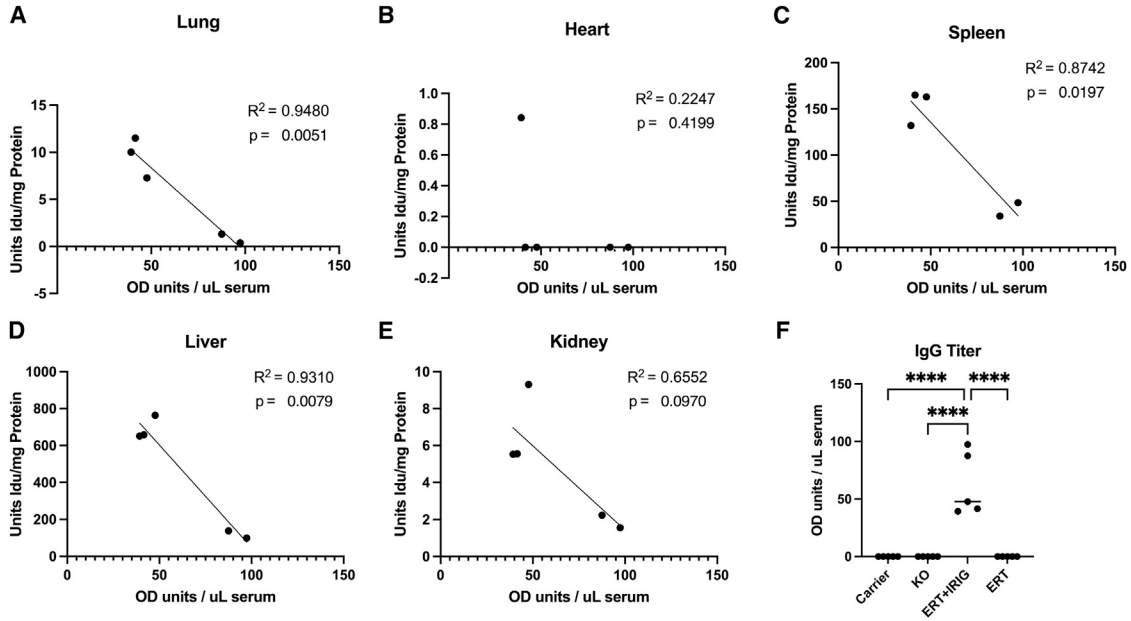

Figure 3. Tissue IDUA activity vs. anti-IDUA IgG titer in ERT+IRIG mice sacrificed at 6 weeks

(A–E) Correlations of IDUA activity to IgG titers in the lungs, heart, spleen, liver, and kidneys, with the R^2 and *p* values shown in the top right corner of each graph. (F) Anti-IDUA IgG antibody titers in mouse serum samples. ELISA was performed at the end of the study in mice sacrificed at 6 weeks. Carrier, untreated carrier NOD-SCID mice; KO, untreated NOD-SCID MPS I KO mice; ERT, NOD-SCID MPS I KO mice treated with weekly i.v. ERT alone; ERT+IRIG, NOD-SCID MPS I KO mice treated with IRIG and weekly IV ERT. $^{*}p < 0.05$, $^{**}p < 0.01$, $^{***}p < 0.001$, $^{****}p < 0.0001$. Each dot represents the measurement from an experimental animal.

recombinant enzyme than the kidneys or lungs, which have been shown to have significant enzyme uptake when administered i.v. to animals, regardless of whether or not antibodies were developed.[8,18,29] The lower IDUA activity and persistent elevation of β-hex in ERT+IRIG-treated mice compared to mice treated with ERT alone in these more difficult-to-treat tissues, while continuing to be effective in the liver and spleen, suggests that there is less ERT efficacy in these tissues when rabbit IgG antibodies against rhIDUA are present, particularly in organs with few reticuloendothelial cells, such as the kidneys and heart, which cannot readily internalize enzyme complexed with IgG antibodies against rhIDUA.

Anti-IDUA antibodies reduce the impact of ERT on cortical bone structure of MPS I mice

We studied the bones of the mice postmortem at age 20 weeks with enzyme activity assays, GAG quantification, and μCT to evaluate biochemical consequences to bone along with cortical and trabecular bone structure from collected femora. The enzyme activity assays displayed that, while whole-bone IDUA activity in both the ERT+IRIG and ERT alone groups was significantly higher than the KO group, there were no significant differences between the two test groups (Figure 4A) (median IDUA activity values: carrier, 2.10 units IDU/mg protein; KO, 0.00 units IDU/mg protein; ERT+IRIG, 7.75 units IDU/mg protein; ERT, 9.60 units IDU/mg protein). When evaluating the β-hex activity from the bones, it was found that carrier and the ERT+IRIG and ERT group values were significantly lower than KO values. Additionally, ERT and carriers were also found to have significantly lower β-hex values when compared to ERT+IRIG and ERT, and Carriers were not significantly different from one another (Figure 4B) (median β-hex activity values: carrier, 897.78 units β-hex/mg protein; KO, 5,227.00 units β-hex/mg protein; ERT+IRIG, 2,218.00 units β-hex/mg protein; ERT, 877.00 units β-hex/mg protein). This indicates, that, since β-hex is used as a measure of efficacy, that ERT without antibodies is more effective on the secondary elevations in MPS I bone disease when compared to ERT+IRIG. Using a Blyscan absorbance assay, GAG levels were also evaluated, and it was found that carriers and the ERT+IRIG and ERT groups all had significantly lower levels of soluble GAGs (sGAGs) when compared to the KO group (Figure 4C). While the ERT-alone groups did not have significantly lower levels of sGAGs when compared to the ERT+IRIG group, the ERT-alone group did display generally lower levels. These results represent ground whole-femur, including bone marrow, which is involved in the reticuloendothelial system and may be leading to the lack of significance between the two treatment groups, as we know from previous studies that the reticuloendothelial system can sequester ERT in the presence of antibodies.[18]

μCT evaluates bone morphology and microarchitecture in mice using X-ray attenuation data acquired at multiple viewing angles to reconstruct a 3D rendition of the sample.[30] Using this rendition, we can then evaluate the cortical and trabecular bone structure of the femur samples. Cortical bone forms ∼90% of the skeleton. This dense bone forms the walls of the shafts of long bones, while trabecular bones

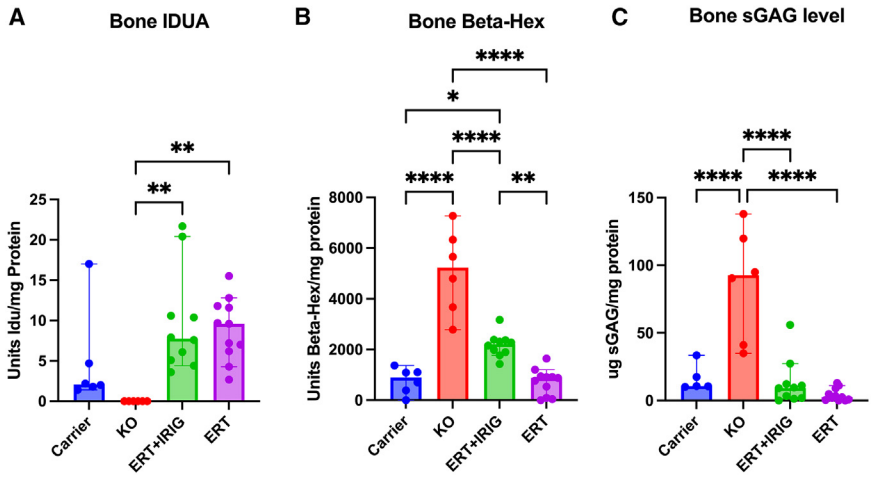

Figure 4. Biochemical analyses from bone homogenate collected from 20-week-old mice

(A) IDUA activity in bone. (B) β-Hex activity in bone. (C) Bone sGAG levels. *$p < 0.05$, **$p < 0.01$, ***$p < 0.001$, ****$p < 0.0001$. Each dot represents the measurement from an experimental animal, and bars symbolize the median value with a 95% CI. Please note differences in scale on the y axis.

make up the inner structure of flat bones and are composed of interconnecting plates and bars that hold the bone marrow.[31,32] Two immune-competent (IC) MPS I (KO) and untreated carrier controls are included in the figures for comparison but are not included in statistical analyses for either trabecular and cortical bone μCT analyses. The untreated MPS I mice showed no significant differences in trabecular bone structure when compared to untreated carrier controls with the exception of bone volume ($p < 0.05$) (Figure 5E). However, untreated MPS I mice did show a higher total cross-sectional area (Tt.Ar), cortical area (Ct.Ar), cortical thickness (Ct.Th), and polar moment of inertia and significantly lower tissue mineral density (TMD) in cortical bone structure when compared to untreated carrier controls (Figures 5E, 6B, 6D, and 6E). With respect to trabecular bone, the groups did not show significant differences to one another (Figures 5E and S1). Images of 3D renderings of the trabecular bone are visually dissimilar to one another, as seen in Figure 5F. In cortical bone, we observed stark differences between mice treated with ERT alone compared with ERT+IRIG (Figures 5 and S2). Mice treated with ERT alone had a cortical bone structure indistinguishable from that of carrier controls, with the exception of TMD values, which were significantly higher in the ERT-alone group compared to all other groups in the study, including carrier controls (ERT alone vs. carrier, $p < 0.01$; ERT alone vs. untreated MPS I and ERT to ERT+IRIG, $p < 0.0001$; Figure 6E). Additionally, when evaluating Tt.Ar, Ct.Ar, Ct.Th, total pore volume (Po.V), average pore volume (Avg-Po.V), standard deviation of pore volume (Po.V.SD), and polar moment of inertia (*J*), mice in the ERT-alone group were observed to have significant (at least $p < 0.05$) differences from the untreated MPS I controls (Figures 6A, 6B, 6D, and 6F–6I). Mice treated with ERT alone also showed significant differences (at least $p < 0.01$) compared to the ERT+IRIG treated mice in Tt.Ar, Ct.Ar, Ct.Th, and *J*, with values in all groups trending closer to carrier controls (Figures 6A, 6B, 6D, and 6I). In contrast to the ERT-alone group, ERT+IRIG-treated mice showed no significant differences in any measurement of cortical bone structure when compared to untreated KO mice. Additionally, carriers and KOs showed significant differences (at least $p < 0.05$) in Ct.Ar., Ct.Th., and TMD (Figures 6B–6D and 6E). Representative images of 3D cortical bone renderings are shown in Figure 6J.

DISCUSSION

Our results suggest that rabbit anti-rhIDUA IgG antibodies interfered with the ability of weekly i.v. ERT that was administered from birth to treat bone disease in MPS I mice. The humoral immune response to ERT has long been suspected to have a clinical impact on the effectiveness of therapy. More than 90% of MPS I patients develop neutralizing antibodies to rhIDUA within the first few months of treatment.[14,29] MPS patients with low titers of inhibitory antibodies are reported to experience fewer upper airway infections compared to patients with higher titers, and increased inhibition of enzyme by antibodies correlates with poorer substrate reduction.[29] While short-term studies on MPS I patient outcomes due to antibody production have been completed, studies of long-term impact of antibodies on disease progression have not been conducted. These studies are challenging to conduct, as anti-rhIDUA antibody titers in patients may wane over time.

One lysosomal disease where the antibody response to ERT has been heavily documented is Pompe disease, a lysosomal storage disorder caused by mutations in the gene encoding the enzyme acid alpha-glucosidase (GAA).[33] GAA is an enzyme that breaks down glycogen in the lysosome, and mutations in GAA lead to accumulation of GAA in a multitude of tissues, with cardiac and skeletal muscles being affected most severely.[33] Patients with classic, infantile-onset Pompe disease (IOPD) present with severe muscle involvement, including cardiomyopathy, hypotonia, and hypoventilation requiring mechanical ventilation, typically within the first 12 months of life.[33] While nearly all Pompe disease patients develop antibodies to ERT, it is most harmful to classic IOPD patients who lack cross-reactive immunological material (CRIM) and develop high antibody titers, after which clinical decline and death occurs despite ERT.[33–35] As a result, patients with classic IOPD who are also CRIM negative are now treated to induce immune tolerance to the ERT prior to treatment with ERT using, most commonly, a combination of rituximab and methotrexate with or without i.v. gamma globulins, and this has led to better long-term clinical outcomes for these patients.[33,35,36] These immune-modulatory treatments can lead to adverse side effects. For instance, methotrexate has been associated with bone marrow and gastrointestinal toxicity after prolonged use, while rituximab has been connected to progressive multifocal leukoencephalopathy and

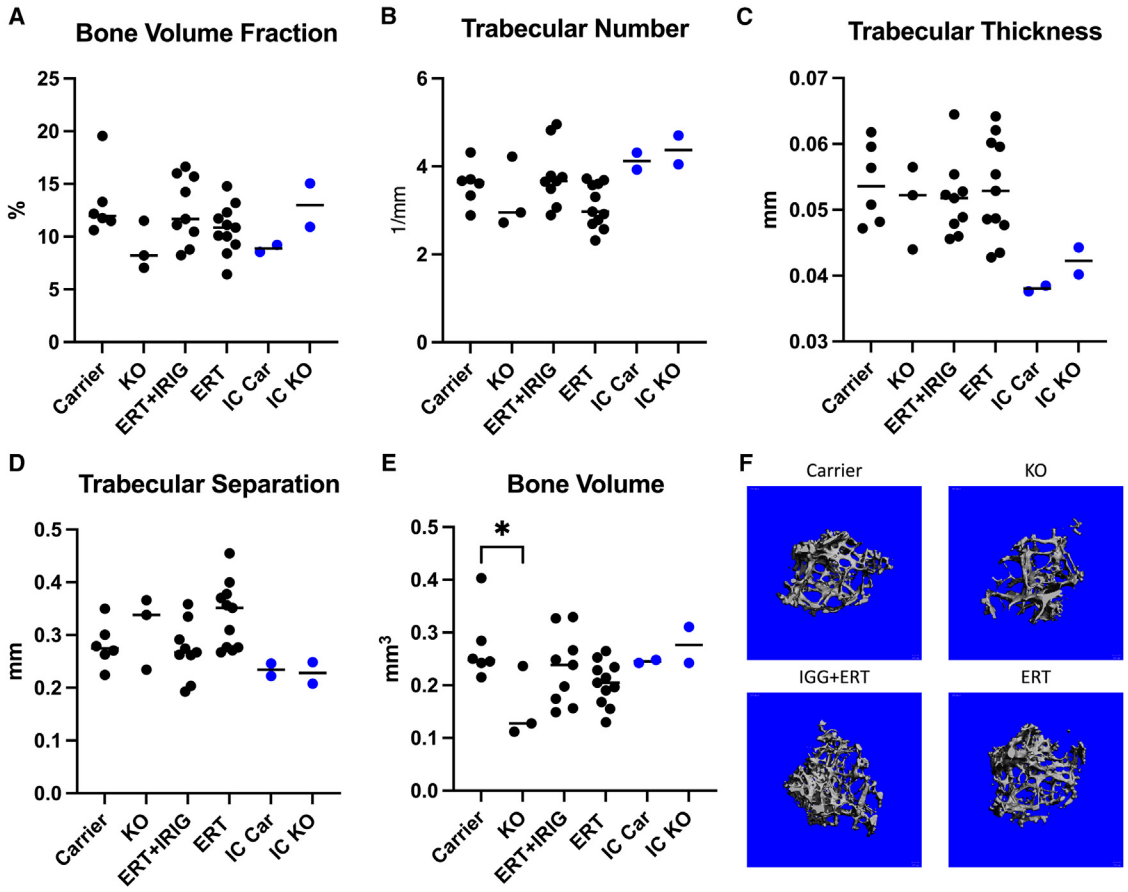

Figure 5. Trabecular bone structure

(A) BV/TV (bone volume fraction). (B) Tb.N (trabecular number). (C) Tb.Th (trabecular thickness). (D) Tb.Sp (trabecular separation). (E) BV (bone volume). (F) Sample μCT images of trabecular bone structure. Carrier, untreated carrier NOD-SCID mice; KO, untreated NOD-SCID MPS I KO mice; ERT+IRIG, NOD-SCID MPS I KO mice treated with IRIG and weekly i.v. ERT; ERT, NOD-SCID MPS I KO mice treated with weekly i.v. ERT alone; IC carrier, immune-competent carrier mice; IC KO, IC MPS I KO mice. Each dot represents a measurement from an experimental animal, and the same animal samples were used for analysis in Figures 5, 6, S1, and S2.

reactivation of previous hepatitis B infection.[37] Other forms of immune modulation have also been connected with nephrotoxicity.[38] As a result, great care must be taken before starting a patient on an immune-modulating protocol. While the immune response to ERT seen in MPS I has not been associated with an increased risk of death, our data suggest that it could be affecting clinical outcomes for patients, including reducing the effectiveness of treatment for skeletal disease.[8,12,18]

The bone disease associated with MPS I leads to some of the most debilitating symptoms for patients.[39] MPS I's bone disease is referred to as dysostosis multiplex and encompasses short stature, thoracolumbar kyphosis, flattened vertebrae, odontoid hypoplasia, short and thick clavicles, and many other skeleton-related MPS I manifestations.[3,39] To understand how these skeletal manifestations occur and how IgG antibodies may be impacting them when ERT is administered, it is important to understand how normal bone growth is interrupted in MPS I. Most bones are formed through endochondral bone formation, in which a cartilage model is formed and slowly replaced by bone matrix made up of mesenchymal cells that differentiate into chondrocytes that produce collagen, attract blood vessels, and direct perichondrial cells into osteoblasts.[39,40] These steps are regulated by signaling molecules called morphogens, including growth factors, which are necessary to ensure correct skeletal formation.[39] Growth factors are important for regulating cell proliferation and adhesion and are necessary for skeletal development.[41] Growth factors are also highly influenced by GAGs. GAGs are transported through the extracellular matrix by translocation to GAG binding sites that enable growth factors to be transferred over large distances until they reach GAGs that act as co-receptors on their targeted cells.[39,42–44] To this end, the large amounts of loose GAGs in the extracellular matrix that are seen in MPS diseases may either be acting to block these necessary growth factors from targeted cells or promote transportation of these growth factors to incorrect cells.[39] GAGs also interact with toll-like receptors and tyrosine kinases, which are necessary for bone remodeling and angiogenesis.[41] GAGs are necessary for

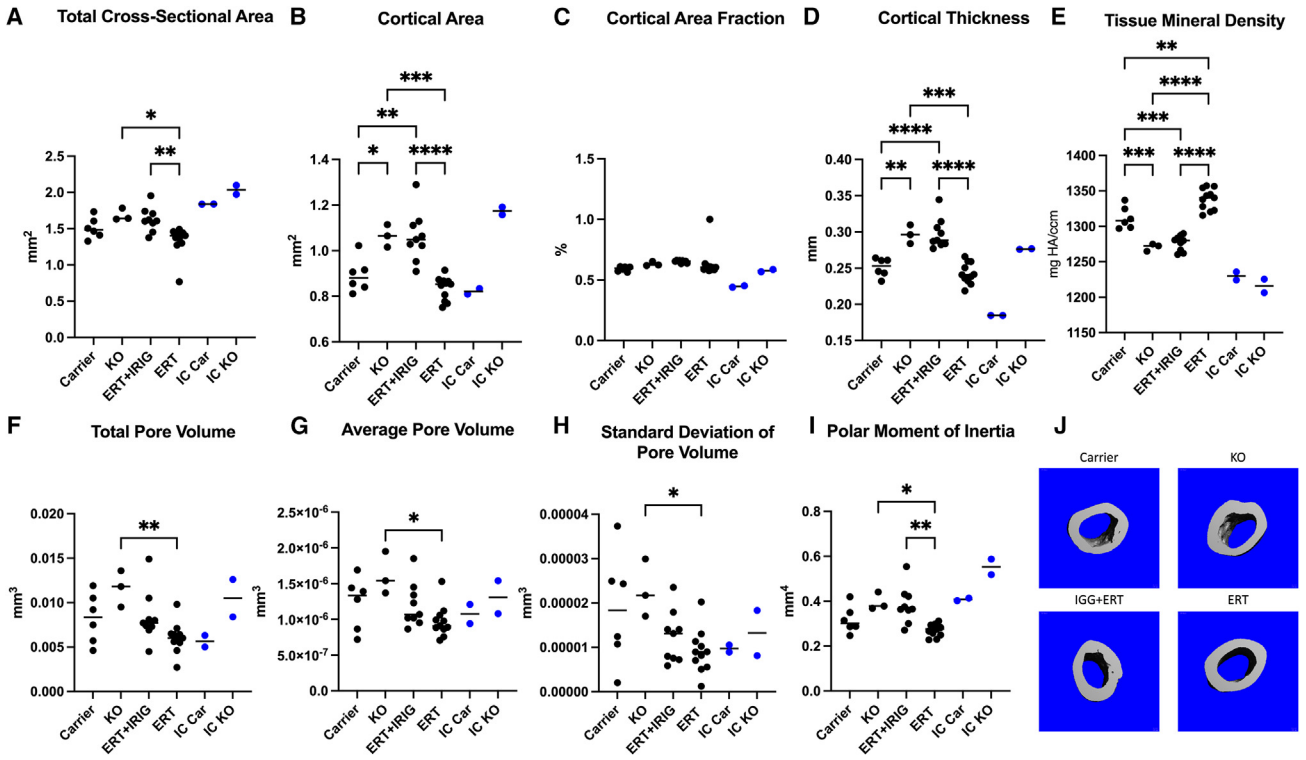

Figure 6. Cortical bone structure

(A) Tt.Ar (total cross-sectional area inside the periosteal envelope). (B) Ct.Ar (cortical area). (C) Ct.Ar/Tt.Ar (Ct.Ar fraction). (D) Ct.Th (cortical thickness). (E) TMD (tissue mineral density). (F) Po.V. (total pore volume). (G) AvgPo.V (average pore volume). (H) Po.V.SD (standard deviation of pore volume). (I and J) (polar moment of Inertia). Shown are sample μCT images of cortical bone structure. CAR, untreated carrier NOD-SCID mice; KO, untreated NOD-SCID MPS I mice; ERT, NOD-SCID MPS I mice treated with weekly i.v. ERT alone; ERT+IRIG, NOD-SCID MPS I mice treated with IRIG and weekly i.v. ERT; IC carrier, IC carrier mice; IC KO, IC KO mice. *$p < 0.05$, **$p < 0.01$, ***$p < 0.001$, ****$p < 0.0001$. Each dot represents the measurement from an experimental animal.

the biomechanics of the extracellular matrix in dynamic tissue structures such as tendons and cartilage, which are altered in MPS I due to GAG accumulation, leading to increased water absorption and abnormal deposition of collagen fibers along with distended cells.[41] However, the full mechanisms leading to MPS skeletal disease are not entirely understood. Some theorize that they may be directly related to altered endochondral ossification.[41] Additionally, growth impairment is believed to be a result of GAGs being deposited in epiphyseal plates.[41,45]

Few studies have shown moderate improvement of skeletal structure upon MPS I murine neonatal administration of ERT.[39] A study in MPS I dogs observed a reduction of inflammation and GAG storage but did not analyze skeletal structure.[46] While ERT alone is able to ameliorate some of the motility and mobility constraints that MPS skeletal and joint disease create for patients, leading to an improvement in growth, endurance, and joint mobility, ERT alone is not able to treat all bone disease phenotypes.[41] It has been shown to improve bone manifestations in combination with ERT or when used on very young, attenuated patients.[41] However, even when treatment is successful, MPS I manifestations still reoccur and require additional interventions.[41] Our results show that the anti-IDUA IgG antibodies that patients and mice receiving ERT develop may be contributing to a lack of effect of the treatment on the bone matrix.[18] The results of this study suggest that combining ERT with an immune suppressant during early life may lead to fewer skeletal deformities for MPS I patients and a better distribution of ERT throughout the body. There could be an additional therapeutic component to immune suppression due to the role of inflammation in the pathogenesis of MPS. Pentosan polysulfate (PPS), a molecule that has prochondral activity and anti-inflammatory properties, has been tested in canine models, where it led to a decrease in GAG accumulation in canines treated with PPS.[41,46] Studies in MPS VI rats have shown a reduction of GAG accumulation in inflammatory markers; using PPS led to an observation of partial rescue of the bone phenotype.[39,47,48] Another study looked into using PPS treatment in conjunction with ERT in adult patients with MPS I and was found to improve hip, knee, and ankle mobility in the patients.[41,49,50]

Our study in newborn mice treated with ERT alone or ERT+IRIG suggests that treatment with ERT from birth may not be sufficient to prevent MPS I skeletal disease in the presence of anti-IDUA antibodies. Potential solutions to explore in clinical studies could include use of an anti-inflammatory drug such as PPS in conjunction with

ERT in newborn patients or implementing induction of immune tolerance prior to administration, similar to what is done for Pompe disease. The skeletal disease MPS I is greatly debilitating for patients, and improving outcomes would be of tremendous benefit. Future studies will be needed to determine whether and how to best prevent the immune response to ERT and the impact it would have on treatment of MPS I disease in human patients.

MATERIALS AND METHODS

Production of IRIG

The rabbit IgG antibodies against rhIDUA used in this study were produced by Thermo Fisher Scientific (Waltham, MA, USA) by immunizing rabbits with rhIDUA. Rabbit sera were tested by uptake inhibition assay[18] before protein A column purification (Thermo Fisher Scientific). The titer of IDUA inhibiting IgG was determined by ELISA as described previously.[18] The ability of the antibodies to block IDUA was determined as outlined in Le et al.[18] The collected antibodies were then stored at −80°C until they were needed for administration to mice.

Administration of ERT and IRIG

NOD-SCID MPS I mice (strain NOD.129(B6)-*Prkdc*^{scid}*Idua*^{tm1Clk}/J; RRID:IMSR_JAX:004083) purchased from The Jackson Laboratory (Bar Harbor, ME, USA) were utilized in this study to ensure that the only immune response was being introduced by the administered rabbit IgG against rhIDUA. Animal experiments conducted as part of this study were approved by the institutional animal care and use committee at LA BioMed (now the Lundquist Institute) (approval number 20551-01). The MPS I genotype was determined using primers (oIMR1451, 5′-GGAACTTTGAGACTTGGAAT GAACCAG-3′; oIMR1452, 5′-CATTGTAAATAGGGGTATCCTT GAACTC-3′; oIMR1453, 5′-GGATTGGGAAGACAATAGCAGG CATGCT-3′). A day before ERT doses, mice were given intraperitoneal (i.p.) injections of IRIG at 22 mg/kg body weight or an equivalent volume of saline for controls. The dose was decided based on the concentration applied in our *in vitro* uptake inhibition assays and converted for *in vivo* studies by the total volume in circulation (data not shown). Doses of 1.57 mg/kg body weight of recombinant IDUA were given i.v. to the ERT+IRIG and ERT-alone groups from birth to the end of the study. To prevent an anaphylaxis reaction, 5 mg/kg diphenhydramine (Hikma Pharmaceutical USA, Berkeley Heights, NJ, USA) was given i.p. before any injections of IRIG, ERT, or saline. ERT was given via facial vein injection at week 0, i.p. from week 1 to week 3, and via tail vein i.v. injection from week 4 onward. Animals were taken down at 6 weeks and 20 weeks as summarized in Table 1. Heart, liver, spleen, kidneys, and lungs were collected for biochemical analyses. Serum samples were collected at 6 weeks for rabbit anti-rhIDUA IgG antibody titers by ELISA. Femora were collected from the 20-week cohort, stripped of soft tissue, and stored at −80°C.

Biochemical analyses

IDUA activity was assessed using 250 μmol/L 4-methylumbelliferyl α-L-iduronide substrate (4-MUI, Glycosynth, Warrington, Cheshire, UK) as described previously,[18,51,52] except that the incubation temperature was 37°C, and the incubation time was 0.5 h. Hexosaminidase activity was assessed using 1.25 mmol/L 4-methylumbelliferyl-*N*-acetyl-β-D-glucosaminide (EMD Millipore, Billerica, MA, USA) substrate with an incubation time of 0.5 h at a temperature of 37°C. Net fluorescence was determined by fluorometry at 365 nm excitation and 440 nm emission. Protein concentrations in the extracts were determined by the Bradford method using reagents from Bio-Rad (Hercules, CA, USA). One unit of enzyme activity is equivalent to a catalytic activity of 1 nmol of 4-MU substrate cleaved per hour at 37°C. Enzyme activity is presented as units/mg protein. A Blyscan assay, a quantitative dye-binding method, was performed to quantify sGAG content in collected bones according to the manufacturer's protocol (Bicolor, Belfast, UK).

μCT

The femora were scanned on a Scanco μCT50 μCT instrument at the Musculoskeletal Research Core at Washington University in St. Louis to analyze cortical and trabecular bone structure. Samples were scanned at 70 kVp, 57 μA, and 4 W using an integration time of 700 ms. The voxel resolution was 7.4 μm. Segmentation thresholds for trabecular bone data were 590 units (low) and 10,000 units (high). For cortical bone data, segmentation thresholds were 620 (low) and 10,000 (high). Only three NOD-SCID MPS I KO samples were available for μCT, and two 20-week-old IC samples for both carrier and KO mice are shown as a comparison to the NOD-SCID mice. IC samples are not included in statistical analyses.

Statistical analysis

Statistical analysis of results was performed using GraphPad Prism (v.10.1.1) (GraphPad, La Jolla, CA, USA) using one-way ANOVA (Figures 3F, 4, 5, 6, S1, and S2) with testing for multiple comparisons using statistical hypothesis testing with Tukey's multiple-comparisons test using a 95% confidence interval. A two-way ANOVA was used for Figure 2 to separate across the different time points, again utilizing Tukey's multiple-comparisons test with a 95% confidence interval. Simple linear regressions were calculated for Figures 3A–3E.

DATA AND CODE AVAILABILITY

The data that support the findings of this study are available from the corresponding author, P.I.D., upon reasonable request, subject to review by BioMarin Pharmaceutical, to ensure there are no commercial restrictions.

ACKNOWLEDGMENTS

Funding was provided by the Eunice Kennedy Shriver National Institute of Child Health and Human Development (R03 HD 074907), the National Science Foundation (NSF) Graduate Research Fellowship Program under award DGE-1745038, and the National Heart, Lung, and Blood Institute (NHLBI) under award F31HL165903. S.-h.K. was supported by a T32 fellowship in the UCLA Medical Genetics Training Program (GM008243). The Washington University Musculoskeletal Research Center is supported by NIH P30 AR074992. rhIDUA in the form of laronidase was provided by BioMarin Pharmaceutical Inc.

AUTHOR CONTRIBUTIONS

P.I.D. and S.Q.L. designed the research studies. S.Q.L., S.-h.K., and Q.D.B. conducted experiments. S.C.H., S.Q.L., S.-h.K., and M.D.B. acquired data. S.C.H., S.Q.L., and S.-h.K. analyzed data. S.C.H. and P.I.D. wrote the manuscript.

DECLARATION OF INTERESTS

The rhIDUA used in the study was provided by BioMarin Pharmaceutical Inc. P.I.D. receives research support from Sanofi Genzyme, Alnylam, and M6P Therapeutics and is consulting for Mandos Health. P.I.D. is a listed inventor on patent USSN 15/946,505; 0WVR-223143-US for enzyme replacement therapy for mucopolysaccharidosis IIID.

SUPPLEMENTAL INFORMATION

Supplemental information can be found online at https://doi.org/10.1016/j.omtm.2024.101405.

REFERENCES

1. Parini, R., Deodato, F., Di Rocco, M., Lanino, E., Locatelli, F., Messina, C., Rovelli, A., and Scarpa, M. (2017). Open issues in Mucopolysaccharidosis type I-Hurler. Orphanet J. Rare Dis. *12*, 112.
2. Clarke, L.A., and Hollak, C.E.M. (2015). The clinical spectrum and pathophysiology of skeletal complications in lysosomal storage disorders. Best Pract. Res. Clin. Endocrinol. Metabol. *29*, 219–235.
3. White, K.K. (2011). Orthopaedic aspects of mucopolysaccharidoses. Rheumatology *50*, v26–v33.
4. Cordes, F.C., and Hogan, M.J. (1942). Dysostosis Multiplex (Hurler's Disease; Lipochondrodysplasia ; Gargoylism): Report of the ocular findings in five cases, with a review of the literature. Arch. Ophthalmol. *27*, 637–664.
5. Cleary, M.A., and Wraith, J.E. (1995). The presenting features of mucopolysaccharidosis type IH (Hurler syndrome). Acta Paediatr. *84*, 337–339.
6. Kobayashi, H., Carbonaro, D., Pepper, K., Petersen, D., Ge, S., Jackson, H., Shimada, H., Moats, R., and Kohn, D.B. (2005). Neonatal gene therapy of MPS I mice by intravenous injection of a lentiviral vector. Mol. Ther. *11*, 776–789.
7. Pievani, A., Azario, I., Antolini, L., Shimada, T., Patel, P., Remoli, C., Rambaldi, B., Valsecchi, M.G., Riminucci, M., Biondi, A., et al. (2015). Neonatal bone marrow transplantation prevents bone pathology in a mouse model of mucopolysaccharidosis type I. Blood *125*, 1662–1671.
8. Dickson, P., Peinovich, M., McEntee, M., Lester, T., Le, S., Krieger, A., Manuel, H., Jabagat, C., Passage, M., and Kakkis, E.D. (2008). Immune tolerance improves the efficacy of enzyme replacement therapy in canine mucopolysaccharidosis I. J. Clin. Invest. *118*, 2868–2876.
9. Ponder, K.P. (2008). Immune response hinders therapy for lysosomal storage diseases. J. Clin. Invest. *118*, 2686–2689.
10. Kakavanos, R., Turner, C.T., Hopwood, J.J., Kakkis, E.D., and Brooks, D.A. (2003). Immune tolerance after long-term enzyme-replacement therapy among patients who have mucopolysaccharidosis I. Lancet *361*, 1608–1613.
11. Xue, Y., Richards, S.M., Mahmood, A., and Cox, G.F. (2016). Effect of anti-laronidase antibodies on efficacy and safety of laronidase enzyme replacement therapy for MPS I: A comprehensive meta-analysis of pooled data from multiple studies. Mol. Genet. Metabol. *117*, 419–426.
12. Langereis, E.J., van Vlies, N., Church, H.J., Geskus, R.B., Hollak, C.E.M., Jones, S.A., Kulik, W., van Lenthe, H., Mercer, J., Schreider, L., et al. (2015). Biomarker responses correlate with antibody status in mucopolysaccharidosis type I patients on long-term enzyme replacement therapy. Mol. Genet. Metabol. *114*, 129–137.
13. Hampe, C.S., Wesley, J., Lund, T.C., Orchard, P.J., Polgreen, L.E., Eisengart, J.B., McLoon, L.K., Cureoglu, S., Schachern, P., and McIvor, R.S. (2021). Mucopolysaccharidosis Type I: Current Treatments, Limitations, and Prospects for Improvement. Biomolecules *11*, 189.
14. Brooks, D.A., Kakavanos, R., and Hopwood, J.J. (2003). Significance of immune response to enzyme-replacement therapy for patients with a lysosomal storage disorder. Trends Mol. Med. *9*, 450–453.
15. Lenders, M., and Brand, E. (2021). Mechanisms of Neutralizing Anti-drug Antibody Formation and Clinical Relevance on Therapeutic Efficacy of Enzyme Replacement Therapies in Fabry Disease. Drugs *81*, 1969–1981.
16. van Kooten, H.A., Ditters, I.A.M., Hoogeveen-Westerveld, M., Jacobs, E.H., van den Hout, J.M.P., van Doorn, P.A., Pijnappel, W.W.M.P., van der Ploeg, A.T., and van der Beek, N.A.M.E. (2022). Antibodies against recombinant human alpha-glucosidase do not seem to affect clinical outcome in childhood onset Pompe disease. Orphanet J. Rare Dis. *17*, 31.
17. Sosa, A.C., Kariuki, B., Gan, Q., Knutsen, A.P., Bellone, C.J., Guzmán, M.A., Barrera, L.A., Tomatsu, S., Chauhan, A.K., Armbrecht, E., and Montaño, A.M. (2020). Oral immunotherapy tolerizes mice to enzyme replacement therapy for Morquio A syndrome. J. Clin. Invest. *130*, 1288–1300.
18. Le, S.Q., Kan, S.H., Clarke, D., Sanghez, V., Egeland, M., Vondrak, K.N., Doherty, T.M., Vera, M.U., Iacovino, M., Cooper, J.D., et al. (2018). A Humoral Immune Response Alters the Distribution of Enzyme Replacement Therapy in Murine Mucopolysaccharidosis Type I. Mol. Ther. Methods Clin. Dev. *8*, 42–51.
19. Dierenfeld, A.D., McEntee, M.F., Vogler, C.A., Vite, C.H., Chen, A.H., Passage, M., Le, S., Shah, S., Jens, J.K., Snella, E.M., et al. (2010). Replacing the Enzyme α-L-Iduronidase at Birth Ameliorates Symptoms in the Brain and Periphery of Dogs with Mucopolysaccharidosis Type I. Sci. Transl. Med. *2*, 60ra89.
20. Hardy, B., Mozes, E., and Danon, D. (1976). Comparison of the immune response potential of newborn mice to T-dependent and T-independent synthetic polypeptides. Immunology *30*, 261–266.
21. Al-Sannaa, N.A., Bay, L., Barbouth, D.S., Benhayoun, Y., Goizet, C., Guelbert, N., Jones, S.A., Kyosen, S.O., Martins, A.M., Phornphutkul, C., et al. (2015). Early treatment with laronidase improves clinical outcomes in patients with attenuated MPS I: a retrospective case series analysis of nine sibships. Orphanet J. Rare Dis. *10*, 131.
22. Gabrielli, O., Clarke, L.A., Ficcadenti, A., Santoro, L., Zampini, L., Volpi, N., and Coppa, G.V. (2016). 12 year follow up of enzyme-replacement therapy in two siblings with attenuated mucopolysaccharidosis I: the important role of early treatment. BMC Med.. Genet. *17*, 19.
23. Pjetraj, D., Santoro, L., Sgattoni, C., Padella, L., Zampini, L., Monachesi, C., Gabrielli, O., and Catassi, C. (2023). 18-year follow-up of enzyme-replacement therapy in two siblings with attenuated mucopolysaccharidosis I. Am. J. Med. Genet. *191*, 564–569.
24. Clarke, L.A., Russell, C.S., Pownall, S., Warrington, C.L., Borowski, A., Dimmick, J.E., Toone, J., and Jirik, F.R. (1997). Murine Mucopolysaccharidosis Type I: Targeted Disruption of the Murine α-l-Iduronidase Gene. Hum. Mol. Genet. *6*, 503–511.
25. Chung, S., Ma, X., Liu, Y., Lee, D., Tittiger, M., and Ponder, K.P. (2007). Effect of neonatal administration of a retroviral vector expressing α-l-iduronidase upon lysosomal storage in brain and other organs in mucopolysaccharidosis I mice. Mol. Genet. Metabol. *90*, 181–192.
26. Kan, S.H., Aoyagi-Scharber, M., Le, S.Q., Vincelette, J., Ohmi, K., Bullens, S., Wendt, D.J., Christianson, T.M., Tiger, P.M.N., Brown, J.R., et al. (2014). Delivery of an enzyme-IGFII fusion protein to the mouse brain is therapeutic for mucopolysaccharidosis type IIIB. Proc. Natl. Acad. Sci. USA *111*, 14870–14875.
27. Wang, D., Shukla, C., Liu, X., Schoeb, T.R., Clarke, L.A., Bedwell, D.M., and Keeling, K.M. (2010). Characterization of an MPS I-H Knock-In Mouse that Carries a Nonsense Mutation Analogous to the Human IDUA-W402X Mutation. Mol. Genet. Metabol. *99*, 62–71.
28. Zheng, Y., Rozengurt, N., Ryazantsev, S., Kohn, D.B., Satake, N., and Neufeld, E.F. (2003). Treatment of the mouse model of mucopolysaccharidosis I with retrovirally transduced bone marrow. Mol. Genet. Metabol. *79*, 233–244.
29. Concolino, D., Deodato, F., and Parini, R. (2018). Enzyme replacement therapy: efficacy and limitations. Ital. J. Pediatr. *44*, 120.
30. Bouxsein, M.L., Boyd, S.K., Christiansen, B.A., Guldberg, R.E., Jepsen, K.J., and Müller, R. (2010). Guidelines for assessment of bone microstructure in rodents using micro–computed tomography. J. Bone Miner. Res. *25*, 1468–1486.
31. Compston, J. (1999). CHAPTER 23 - Histomorphometric Manifestations of Age-Related Bone Loss. In The Aging Skeleton, C.J. Rosen, J. Glowacki, and J.P. Bilezikian, eds. (San Diego: Academic Press), pp. 251–261.
32. Christensen, A.M., Passalacqua, N.V., and Bartelink, E.J. (2014). Chapter 2 - Human Osteology and Odontology. In Forensic Anthropology, A.M. Christensen, N.V. Passalacqua, and E.J. Bartelink, eds. (San Diego: Academic Press), pp. 19–53.

33. Kohler, L., Puertollano, R., and Raben, N. (2018). Pompe Disease: From Basic Science to Therapy. Neurotherapeutics *15*, 928–942.

34. Banugaria, S.G., Prater, S.N., Patel, T.T., DeArmey, S.M., Milleson, C., Sheets, K.B., Bali, D.S., Rehder, C.W., Raiman, J.A.J., Wang, R.A., et al. (2013). Algorithm for the Early Diagnosis and Treatment of Patients with Cross Reactive Immunologic Material-Negative Classic Infantile Pompe Disease: A Step towards Improving the Efficacy of ERT. PLoS One *8*, e67052.

35. Messinger, Y.H., Mendelsohn, N.J., Rhead, W., Dimmock, D., Hershkovitz, E., Champion, M., Jones, S.A., Olson, R., White, A., Wells, C., et al. (2012). Successful immune tolerance induction to enzyme replacement therapy in CRIM-negative infantile Pompe disease. Genet. Med. *14*, 135–142.

36. Doerfler, P.A., Nayak, S., Corti, M., Morel, L., Herzog, R.W., and Byrne, B.J. (2016). Targeted approaches to induce immune tolerance for Pompe disease therapy. Mol. Ther. Methods Clin. Dev. *3*, 15053.

37. Banugaria, S.G., Patel, T.T., and Kishnani, P.S. (2012). Immune modulation in Pompe disease treated with enzyme replacement therapy. Expet Rev. Clin. Immunol. *8*, 497–499.

38. de Mattos, A.M., Olyaei, A.J., and Bennett, W.M. (2000). Nephrotoxicity of immunosuppressive drugs: Long-term consequences and challenges for the future. Am. J. Kidney Dis. *35*, 333–346.

39. Kingma, S.D.K., and Jonckheere, A.I. (2021). MPS I: Early diagnosis, bone disease and treatment, where are we now? J. Inherit. Metab. Dis. *44*, 1289–1310.

40. Jiang, Z., Lau, Y.K., Wu, M., Casal, M.L., and Smith, L.J. (2021). Ultrastructural analysis of different skeletal cell types in mucopolysaccharidosis dogs at the onset of postnatal growth. J. Anat. *238*, 416–425.

41. De Ponti, G., Donsante, S., Frigeni, M., Pievani, A., Corsi, A., Bernardo, M.E., Riminucci, M., and Serafini, M. (2022). MPSI Manifestations and Treatment Outcome: Skeletal Focus. Int. J. Mol. Sci. *23*, 11168.

42. De Pasquale, V., and Pavone, L.M. (2019). Heparan sulfate proteoglycans: The sweet side of development turns sour in mucopolysaccharidoses. Biochim. Biophys. Acta, Mol. Basis Dis. *1865*, 165539.

43. Cortes, M., Baria, A.T., and Schwartz, N.B. (2009). Sulfation of chondroitin sulfate proteoglycans is necessary for proper Indian hedgehog signaling in the developing growth plate. Dev. Camb. Engl. *136*, 1697–1706.

44. Vyas, N., Goswami, D., Manonmani, A., Sharma, P., Ranganath, H.A., Vijay Raghavan, K., Shashidhara, L.S., Sowdhamini, R., and Mayor, S. (2008). Nanoscale organization of hedgehog is essential for long-range signaling. Cell *133*, 1214–1227.

45. Viskochil, D., Clarke, L.A., Bay, L., Keenan, H., Muenzer, J., and Guffon, N. (2019). Growth patterns for untreated individuals with MPS I: Report from the international MPS I registry. Am. J. Med. Genet. *179*, 2425–2432.

46. Simonaro, C.M., Tomatsu, S., Sikora, T., Kubaski, F., Frohbergh, M., Guevara, J.M., Wang, R.Y., Vera, M., Kang, J.L., Smith, L.J., et al. (2016). Pentosan Polysulfate: Oral Versus Subcutaneous Injection in Mucopolysaccharidosis Type I Dogs. PLoS One *11*, e0153136.

47. Frohbergh, M., Ge, Y., Meng, F., Karabul, N., Solyom, A., Lai, A., Iatridis, J., Schuchman, E.H., and Simonaro, C.M. (2014). Dose responsive effects of subcutaneous pentosan polysulfate injection in mucopolysaccharidosis type VI rats and comparison to oral treatment. PLoS One *9*, e100882.

48. Schuchman, E.H., Ge, Y., Lai, A., Borisov, Y., Faillace, M., Eliyahu, E., He, X., Iatridis, J., Vlassara, H., Striker, G., and Simonaro, C.M. (2013). Pentosan Polysulfate: A Novel Therapy for the Mucopolysaccharidoses. PLoS One *8*, e54459.

49. Hennermann, J.B., Gökce, S., Solyom, A., Mengel, E., Schuchman, E.H., and Simonaro, C.M. (2016). Treatment with pentosan polysulphate in patients with MPS I: results from an open label, randomized, monocentric phase II study. J. Inherit. Metab. Dis. *39*, 831–837.

50. Polgreen, L.E., Kunin-Batson, A., Rudser, K., Vehe, R.K., Utz, J.J., Whitley, C.B., and Dickson, P. (2017). Pilot study of the safety and effect of adalimumab on pain, physical function, and musculoskeletal disease in mucopolysaccharidosis types I and II. Mol. Genet. Metab. Rep. *10*, 75–80.

51. Ou, L., Herzog, T.L., Wilmot, C.M., and Whitley, C.B. (2014). Standardization of α-L-iduronidase Enzyme Assay with Michaelis-Menten Kinetics. Mol. Genet. Metabol. *111*, 113–115.

52. Wendeler, M., and Sandhoff, K. (2009). Hexosaminidase assays. Glycoconj. J. *26*, 945–952.